PHYSICAL REVIEW B VOLUME 54, NUMBER 15 15 OCTOBER 1996-I

First-principles theoretical study of metallic states of DCNQI-(Cu,Ag,Li) systems

Tsuyoshi Miyazaki* and Kiyoyuki Terakura
Joint Research Center for Atom Technology, National Institute for Advanced Interdisciplinary Research,
1-1-4 Higashi, Tsukuba, Ibaraki 305, Japan

(Received 16 February 1996)

The detailed electronic structures of several materials of organic solids, $(R_1,R_2\text{-DCNQI})_2M$, were studied with the first-principles method based on the local-density approximation supplemented by the generalized gradient approximation. The present calculations account well for the qualitative differences in the electronic properties produced by different metal cations (M=Li, Ag, and Cu). Unique aspects of the systems with $R_1=R_2=\mathrm{I}$ are also explained based on the present calculations. The very small hole Fermi surface observed by the de Haas–van Alphen measurement for $(\text{DMe-DCNQI})_2\text{Cu}$ was well reproduced by the calculation with the observed crystal structure. [S0163-1829(96)02939-6]

I. INTRODUCTION

Organic solids, especially the conducting ones, form one of the most attractive categories of materials. Organic solids belong to molecular crystals, in general. In contrast to some examples of simple molecular crystals such as H_2, N_2, Cl_2, and so on, the constituent molecules in organic solids are rather complex and a variety of modifications of the molecules are possible even with only a few kinds of elements involved. This leads to very rich variety in organic solids. Many of the organic molecules are planar in shape and they are stacked face to face to form solids. Therefore, physical properties show a strong anisotropy with respect to the direction of stacking molecules. Very often they show strong one-dimensional (1D) character, which is very suitable for studying physics of 1D systems. However, 1D systems become insulating at low temperatures due to the Peierls transition even if they are metallic at higher temperatures. Therefore, in order to maintain the conducting state at low temperatures particularly aiming to realize superconductivity, efforts have been made to add three dimensionality to organic solids. The DCNQI (dicyanoquinonediimine) systems have very unique aspects with regard to dimensionality although none of them has shown superconductivity so far.[1–4]

In the molecular crystals, the constituent molecules keep essentially the characters of isolated molecules because intermolecular interactions are generally much weaker than the intramolecular interactions. Therefore, even in the solids, the electronic structures near the Fermi level are mostly determined by highest occupied molecular orbital (HOMO) and lowest unoccupied molecular orbital (LUMO) of the constituent molecules. This is a justification for the use of the tight-binding (TB) Hückel approximation to analyze the electronic properties of molecular crystals. In fact, there are several examples where such a simple analysis works very well.[5,6]

However, in organic solids, the constituent molecules are generally large and as a molecule becomes larger, the energy separation between intramolecular levels becomes smaller. There is no guarantee *a priori* that the intermolecular interaction is smaller than the intramolecular HOMO-LUMO energy separation and therefore no guarantee either for the validity of the TB Hückel approximation. Another problem of the TB Hückel approximation, in general, is that there are some parameters to be determined empirically by using experimental data. However, if we aim to study really new materials, relevant experimental data may not be available. For these reasons, it is highly desired to check the capability of the first-principles calculations to describe the electronic structures of organic solids.

The electronic structure calculations based on local-density approximation[7] (LDA) and recently generalized gradient approximation[8] (GGA) have been playing important roles in the physics and chemistry of inorganic solids. However, because of the complexity of the structure, it has been rather difficult to perform such calculations with the same order of accuracy for organic solids. Organic solids are covalently bonded systems with many atoms and with low symmetry. The efficient methods based on the muffin-tin potential or atomic sphere approximation, for example linear muffin-tin orbital)[9] (LMTO) or augmented spherical wave[10] (ASW) method, are not accurate enough to describe the wave functions of low-symmetry systems. In fact, Kübler *et al.* performed *ab initio* calculations for β-$(\text{BEDT-TTF})_2\text{I}_3$ by ASW method,[11] but they could not correctly reproduce the Fermi surface observed by experiments, while a semiempirical method gave a much better result.[5] On the other hand, the ordinary pseudopotential method is not efficient for describing the electronic states of the first-row elements which are always contained in organic solids, because pseudopotentials of $2p$ orbitals for these elements are deep and many plane waves are needed to describe these orbitals accurately.

Two major progresses in the computational methods have overcome the difficulties mentioned above. First, Car and Parrinello introduced a computational method for the molecular dynamics based on the electronic structure calculation.[12] Subsequent analyses clarified the fact that the Car-Parrinello method provides also an efficient algorithm for the electronic structure calculation itself. It is, of course, important that the Car-Parrinello method enables us to do efficient structural optimization. Several improvements have been made to the Car-Parrinello method to enhance the efficiency. Second, Vanderbilt proposed a formalism in the pseudopotential theory.[13] He pointed out that the constraint of norm conservation is not necessary for constructing pseudo wave functions. This pseudopotential called ultrasoft pseudopotential reduces the number of plane waves significantly for the first-row elements and 3*d* transition-metal elements.

In the present work, we have calculated the electronic structures of $(2,5\text{-}R_1,R_2\text{-DCNQI})_2M$ by using the modified Car-Parrinello method and the ultrasoft pseudopotential. R_1 and R_2 are substituents of a DCNQI molecule and M a metallic element. We will demonstrate, in this paper, that the theoretical study of organic solids based on the first-principles calculations is now in the same level of reliability as that for inorganic solids.[14,15] We have studied several materials obtained by different combinations of R_1, R_2, and M: $R_1 = R_2 = \text{CH}_3$, Br, and I; $M =$ Li, Ag, and Cu. The present calculation accounts well for the similarity and the difference among these materials.

All the crystal structures used in the present work are taken from experiments. However, it is now possible to determine the crystal structure fairly accurately by the first-principles electronic structure calculation. Theoretical structure determination has been playing crucial roles in aperiodic systems and will also play important roles for organic materials whose crystal structures are hard to determine experimentally in several circumstances. In the next paper, we will discuss the accuracy of the theoretical structure determination.

This paper is organized as follows. In Sec. II, we will review the experimental backgrounds. Section III is devoted to a description of the details of the calculations. The results and discussion are given in Sec. IV. Finally, Sec. V is for concluding remarks.

II. EXPERIMENTAL BACKGROUNDS

The molecular structure of the planar molecule 2,5-R_1, R_2-DCNQI is shown in Fig. 1. In $(2,5\text{-}R_1,R_2\text{-DCNQI})_2M$, the molecules DCNQI are acceptors and are stacked face to face along one direction as in many other organic conductors. For Cu, Ag, and Li as a cation M, the crystal is isostructural with the space group $I4_1/a$ as shown in Fig. 2. The bravais lattice of the crystal structure is body-centered tetragonal and the lattice parameters of $a \sim 21$ Å and $c \sim 4$Å suggest strong anisotropy particularly in the transport properties. The main direction of electron conduction is parallel to the c axis, which is the stacking direction of DCNQI molecules. These 1D columns of DCNQI molecules are connected to each other by the cation M through cyano groups at the end of molecules. The cation M is coordinated by N atoms with a local symmetry of D_{2d}, i.e., in a distorted tetrahedral fashion.[1] The angle α in Fig. 3, which ranges from 122° to 127° for Cu salts, indicates the degree of distortion from the T_d symmetry ($\alpha \sim 109°$). Some of the structural data of the systems treated in this paper are listed in Table I.

Although the crystal structure is almost the same, physical properties strongly depend on the choice of M. In the case of Ag and Li salts, they show very strong 1D characters. Most of them are metallic at room temperature and it becomes insulating at lower temperatures. The fact that the change of the conductivity around the metal-insulator (MI) transition is continuous suggests that the transition is of second order. This transition is associated with the Peierls transition with the $2k_F$ instability which produces a charge density wave (CDW) with fourfold periodicity. The appearance of fourfold periodicity is easy to understand. As both of Li and Ag take $+1$ charge state, the charge state of a DCNQI molecule is -0.5 leading to quarter-filled 1D bands formed by DCNQI LUMO orbitals with the Fermi wave vector $k_F = (\pi/4c)$. Therefore, the $2k_F$ instability produces fourfold periodicity along the c axis.

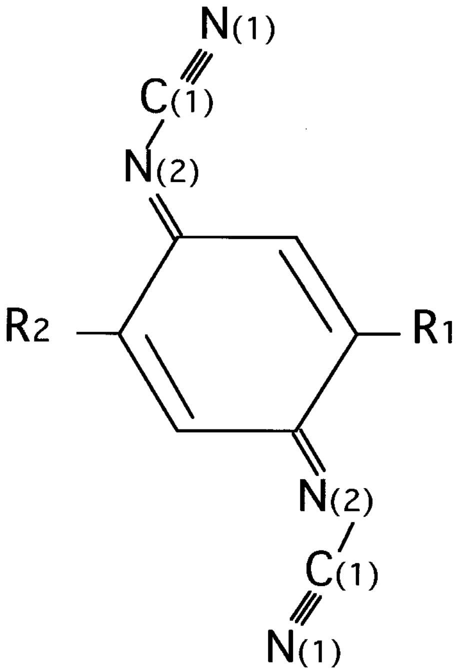

FIG. 1. Molecular structure of the R_1,R_2-DCNQI molecule.

However, there is another important aspect to be noted. According to Moret[16] for the Ag salt, the $4k_F$ instability occurs at 100 K, which is followed by the $2k_F$ instability at 83 K. This implies that the electron-electron interaction is important in the DCNQI LUMO bands. The general features of Ag and Li salts mentioned above are insensitive to the choice of R_1 and R_2.

On the other hand, properties of Cu salts strongly depend on their substituents R_1 and R_2 and are categorized into three groups.[2–4] For example, $(\text{DMe-DCNQI})_2\text{Cu}$ with $R_1 = R_2 = \text{CH}_3$ (Me) and $(\text{DI-DCNQI})_2\text{Cu}$ with $R_1 = R_2 = \text{I}$ belong to the group I and they are metallic in ambient pressure down to very low temperatures (≤ 1 K). The group II materials, some examples of which are $(\text{DBr-DCNQI})_2\text{Cu}$ and completely deuterated $(\text{DMe-DCNQI})_2\text{Cu}$,[4,17] show a metal-insulator transition. Some $(\text{DMe-DCNQI})_2\text{Cu}$ materials with selective deuteration[18] belong to the group III and they show successive phase transitions, metal→insulator→metal, as the decrease of temperature. There is another unique aspect that the group I materials are converted to the group II or III materials by applying pressure. For example, $(\text{DMe-DCNQI})_2\text{Cu}$ becomes a group III material only by applying pressure higher than 100 bar.[19] This means the unusual fact that the insulating phase becomes more stable under pressure.

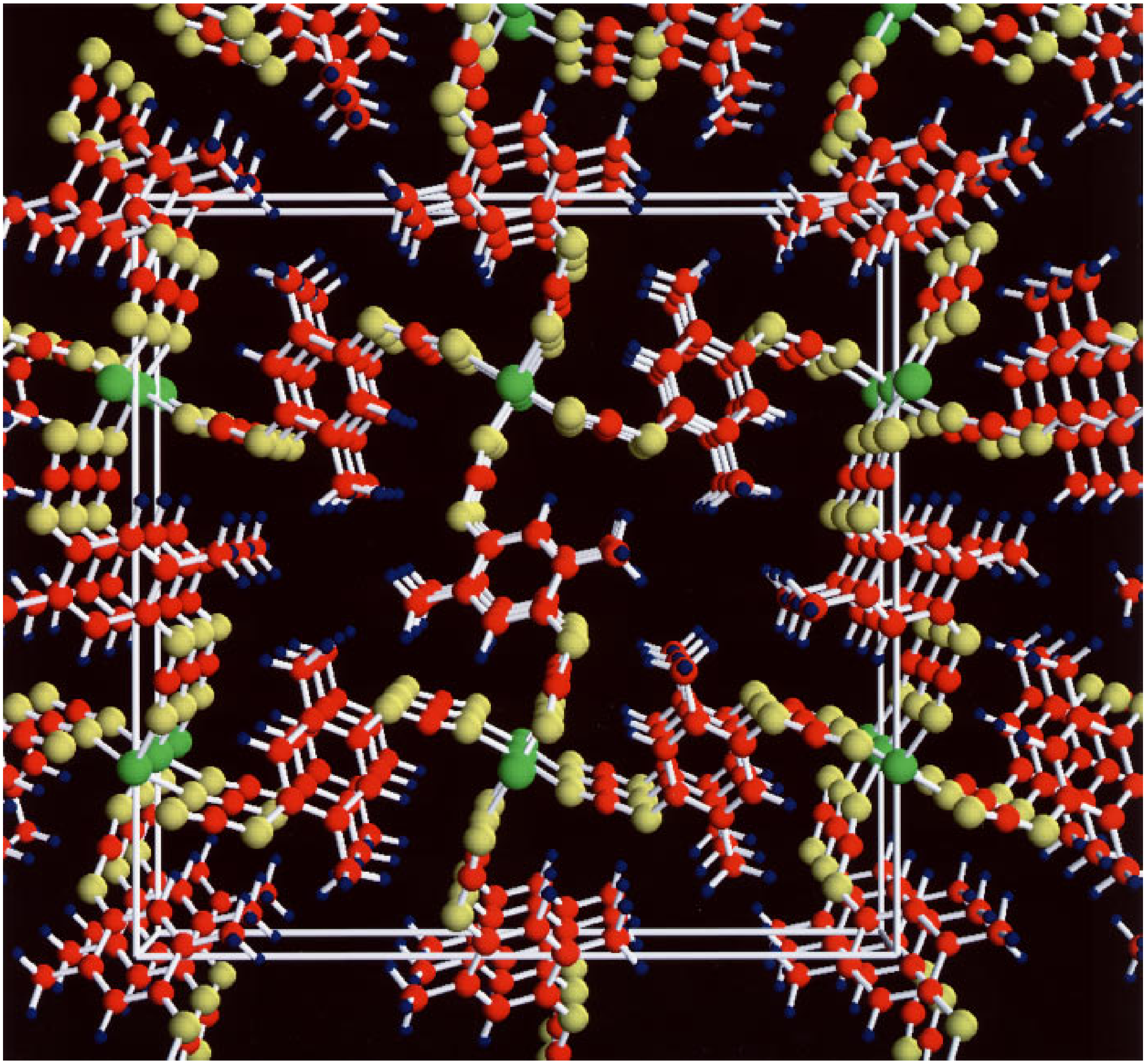

FIG. 2. A stereo view along the c axis of a crystal structure of $(R_1,R_2\text{-DCNQI})_2M$.

The metallic states of Cu salts show some 3D characters in their transport properties.[20] The 3D character was also confirmed by de Haas–van Alphen (dHvA) measurements[6] and by polarized reflectance spectra.[21] The MI transition is accompanied with the CDW formation with threefold periodicity along the c axis. In contrast to the fourfold periodicity in the Li and Ag salts, the threefold periodicity in the Cu salt cannot be explained in simple terms. In the insulating phase, a charge ordering of Cu, Cu^{2+}-Cu^{1+}-Cu^{1+}-Cu^{2+}-$\cdots$, is observed and Cu^{2+} is supposed to have a localized spin magnetic moment. In fact, the susceptibility shows a Curie-Weiss behavior in the insulating phase. Most Cu salts are supposed to have qualitatively the same insulating and metallic phases and have similar phase diagrams except $(\text{DI-DCNQI})_2\text{Cu}$.

Among several Cu salts, $(\text{DI-DCNQI})_2\text{Cu}$ shows unique physical properties. $(\text{DI-DCNQI})_2\text{Cu}$ belongs to group I and its metallic state is much more stable against pressure than $(\text{DMe-DCNQI})_2\text{Cu}$. The critical pressure of 15 kbar[22] is the highest among Cu salts at the present stage. The most unique aspect of $(\text{DI-DCNQI})_2\text{Cu}$ is that it has another metallic phase under higher pressures than 20 kbar.[22] This metallic phase has not been observed in other Cu salts. Very recently it has been reported that there are additional phases under higher pressures in $(\text{DI-DCNQI})_2\text{Cu}$.[23] Moreover, the metallic states of $(\text{DI-DCNQI})_2\text{Cu}$ at ambient pressure are also unique: the temperature dependence of resistivities and susceptibilities[24] are different from those of other Cu salts, the anisotropy of the conductivities is very small,[22] and the electronic specific heat coefficient γ of 75 $\mathrm{mJ/mol\,K^2}$ is three times or even larger than that for $(\text{DMe-DCNQI})_2\text{Cu}$.[25] It is suggested that the electron correlation is important in this system. The uniqueness of I as substituents is seen not only in the Cu salt, but also in the Li and Ag salt. $(\text{DI-DCNQI})_2\text{Li}$ and $(\text{DI-DCNQI})_2\text{Ag}$ show semiconducting behavior in its electronic conductivities even at room tem-

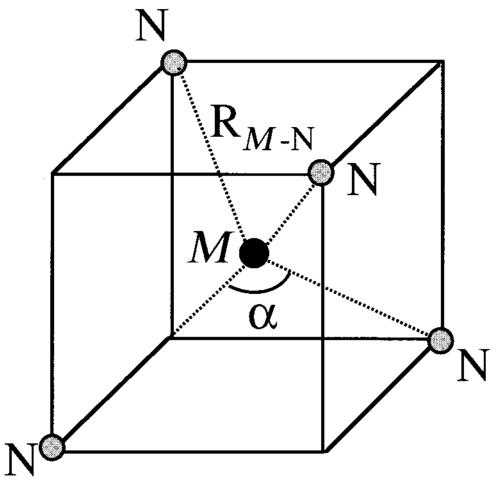

FIG. 3. The coordination geometry of a cation M with its nearest nitrogen atoms. $R_{M-\mathrm{N}}$ denote the bond length between the cation M and the nitrogen atom. The bond angle $\angle \mathrm{N}M\mathrm{N}$ is represented by α.

perature, and no superstructures have been reported.[26] Moreover, their magnetic behavior at low temperatures is different from other Li and Ag salts.[27]

Judging from the experimental facts described in the above, we can set the following aspects as targets of our theoretical study:

(1) threefold periodicity of the CDW in the Cu salt,

(2) whether or not the first-principles calculation can reproduce the tiny hole Fermi surface at the Γ point observed experimentally,

(3) qualitative difference between the Ag and Cu salts,

(4) uniqueness of I as substituents R_1,R_2 in both Cu salts and Li salts.

III. COMPUTATIONAL DETAILS

The present calculation is based on GGA (Ref. 8) in the density functional theory, while the LDA was used in our previous work.[14] We adopt the GGA here in order to maintain the consistency between the present calculation and the structure optimization in the next paper. It is known that the accuracy in the theoretical structure determination is improved by the GGA particularly for systems containing the first-period elements and 3*d* transition-metal elements. The difference in the electronic structure between the LDA and the GGA is almost negligible if we use the same lattice parameters and atomic coordinates. The functional of exchange-correlation part is taken from Ref. 8.

In the present calculations, ultrasoft pseudopotentials are used for the *p* states of C and N, the *d* states of Cu and Ag, and *s* state of H. For other states, we employ the optimized norm-conserving pseudopotentials.[28] The cutoff energy in the wave functions used in most calculations is 25 Ry. This value is determined mainly by the requirement for generating reliable pseudopotentials of C and N. In $(\mathrm{DCNQI})_2M$, there is a very short bond length of C-N (~1.16 Å) at the end of the DCNQI molecule. Therefore, small core radii have to be adopted for C and N resulting in a large cutoff energy for the wave functions. On the other hand, the cutoff energy of 196 Ry in the plane-wave expansion of the charge density is needed to describe the deficit charge[13] for 3*d* orbitals of Cu properly. For some systems we compared the band structure obtained by using 36 Ry as a cutoff energy with that by using 25 Ry, both calculations being performed by using a small number of *k* points, and found that the difference was negligible. As for the *k* point sampling, 19 irreducible *k* points in 1/8 of the first Brillouin zone are used in the self-consistent calculations. To obtain the precise band structure near the Fermi level eigenenergies of some additional *k* points are calculated by using the charge density obtained by the self-consistent calculations. A tetrahedron method is adopted to estimate the Fermi energy accurately. In the case of DMe salts there are 90 atoms in the unit cell with two formula units and there are about 150 band branches only for the valence states for Ag and Cu salts. We take 155 band branches for the self-consistent calculations in the case of $M=\mathrm{Cu}$ and Ag. Due to the large unit cell size, about 13,000 plane waves are needed to expand a wave function for each band and each *k* point.

In order to produce the Fermi surface in detail, the band structure at many *k* points has to be obtained. The first-principles calculation for many *k* points, enough to produce detailed Fermi surfaces is practically not feasible for this kind of complex system at the present stage. Therefore, we fit the band structure obtained by the first-principles calculation with a simple TB model. This fitting can be done with high accuracy, except for $(\mathrm{DI\text{-}DCNQI})_2\mathrm{Cu}$.

IV. RESULTS AND DISCUSSION

In this section, we present calculated results and discuss the differences of the electronic structures between different choices of R_1, R_2, and M.

A. $(\mathrm{DMe\text{-}DCNQI})_2\mathrm{Ag}$ and $(\mathrm{DMe\text{-}DCNQI})_2\mathrm{Li}$

Before discussing solids we show the LUMO of a DMe-DCNQI molecule in Fig. 4. The LUMO has an antibonding

TABLE I. Some of the structural data for systems $(R_1,R_2\text{-DCNQI})_2M$ treated in this paper. a and c are lattice parameters. α is shown in Fig. 3. $R_{M-\mathrm{N}}$ is the bond length between cation M and its nearest N atom.

M	Ag	Li		Cu		
$R_1=R_2$	Me (Ref. 29)	Me (Ref. 29)	I (Ref. 26)	Me (Ref. 4)	Br (Ref. 1)	I (Ref. 26)
a (Å)	22.348	21.901	21.961	21.654	21.558	21.759
c (Å)	3.818	3.788	3.991	3.792	3.896	4.004
α (degree)	128.34	128.31	125.8	126.3	125.3	123.27
$R_{\mathrm{M-N}}$ (Å)	2.306	2.051	2.060	1.972	1.973	1.989

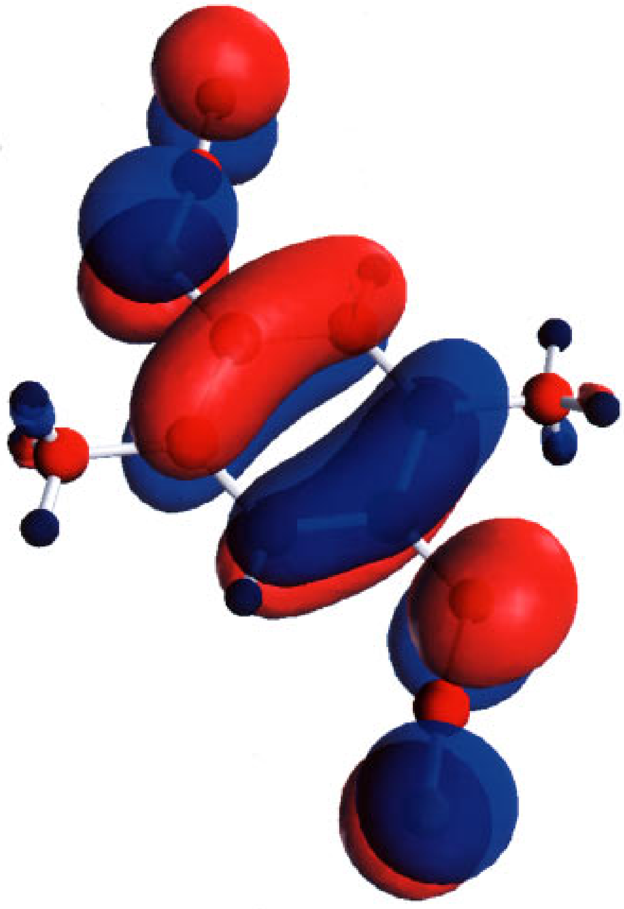

FIG. 4. The LUMO wave function of a DMe-DCNQI molecule. The red (blue) part indicates the region where the wave function has the positive (negative) sign.

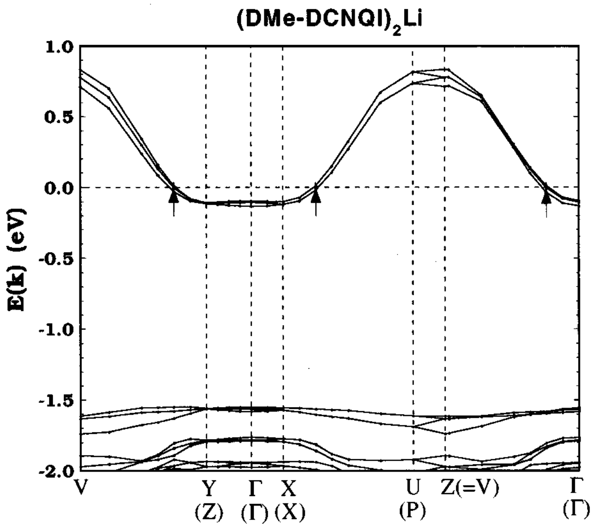

FIG. 5. Band structures of (DMe-DCNQI)$_2$Li. The labeling in k space according to Ref. 40 is also shown in parentheses. The origin of energies is taken at the Fermi level. The arrows along the horizontal dotted line indicate the Fermi wave vector corresponding to the CDW formation with fourfold periodicity along the c axis.

character with the nodes of its wave function in the DCNQI molecular plane and its wave function has a significant weight on the N atom at the end of the molecule, which is the nearest neighbor atom of a cation in the solids (DCNQI)$_2M$. It should be noted that the LUMO has little weight on methyl radicals.

Figure 5 shows the band structure near the Fermi level for (DMe-DCNQI)$_2$Li. The corresponding one for (DMe-DCNQI)$_2$Ag is almost the same as the one shown in Fig. 5(b) of Ref. 14, although the former and the latter were obtained by a GGA and a LDA, respectively. The atomic coordinates and lattice parameters used in the calculations are those of the metallic phase and determined by experiments at room temperature for Ag and 118 K for Li salt.[29] In both salts the Fermi level is located within the four LUMO bands which come mainly from the LUMO's of (DMe-DCNQI) molecules. These four LUMO bands are almost degenerate and they have very weak dispersions along the direction perpendicular to the c axis (along the $Y\Gamma$ and ΓX lines), while the width of the bands along the direction parallel to the c axis (VY, XU, and $Z\Gamma$ lines) is about 0.9 eV and the shape the bands is essentially a 1D cosine type. Although there are some differences in the shape of the bands along the direction perpendicular to the c axis, Ag and Li salts have qualitatively the same LUMO bands. The above results suggest that both Ag and Li salts have a strong 1D character in the transport properties and this is consistent with the experimental results.

The d levels of a cation M should split into two levels e_g ($d_{3z^2-r^2}$ and $d_{x^2-y^2}$) and t_{2g} (d_{xy}, d_{yz} and d_{zx}) if the crystal field at the cation M site is determined only by the four nearest N atoms and the coordination of the four N atoms has the T_d symmetry. In (DCNQI)$_2M$, the N atom coordination is distorted from T_d symmetry and has the local symmetry of D_{2d}. Thus, the high-lying t_{2g} states split into two levels d_{xy} and (d_{yz}, d_{zx}) whose energy split is determined by the angle α in Fig. 3. In Fig. 5(b) of Ref. 14, the two bands about 0.6 eV below the bottom of the LUMO bands come mainly from the d_{xy} states of Ag. The four bands of the d_{yz} and d_{zx} origin are located about 0.5 eV below the d_{xy} bands and the $d_{3z^2-r^2}$,$d_{x^2-y^2}$ states merge into the HOMO bands. The band structure near the Fermi level can be well reproduced by the TB model calculation. All d orbitals are included in the present TB fit in order to reproduce the detailed band structures near the Fermi level. Table II shows some of the fitting parameters. The projected density of states (DOS's) for each orbital of the Ag salt is calculated by this TB fit and is shown in Fig. 6, while the total DOS's is obtained by the original band structure. The mixing of d states into the LUMO bands is fairly small but not negligible. By using the projected DOS's in Fig. 6, the charge state of Ag is estimated to be 1.19, while its formal value is 1.0.

Four Fermi surfaces obtained by these band structures are almost planar because of their strong 1D characters implying the instability of nesting along the c axis. As was mentioned in the previous section, the four LUMO bands are a quarter filled on average. The fact that the four LUMO bands are almost degenerate leads to the result $2k_F \sim \frac{1}{4}c^*$ for all four LUMO bands with c^* the reciprocal lattice constant in the c direction. The arrows in Figs. 5 and in Fig. 5(b) of Ref. 14 denote the Fermi wave vector corresponding to the CDW formation with fourfold periodicity along the c axis.

TABLE II. Some of the fitted parameters in the TB model (in eV).

	(DMe-DCNQI)$_2$Ag	(DMe-DCNQI)$_2$Cu	(DBr-DCNQI)$_2$Cu	(DI-DCNQI)$_2$Cu
Hopping integrals				
LUMO-LUMO (interchain)	-0.01	-0.01	-0.02	-0.03
LUMO-LUMO (intrachain)	-0.22	-0.25	-0.18	-0.14
LUMO -d_{xy}	0.13	0.12	0.12	0.11
LUMO -d_{yz}	-0.04	-0.04	-0.03	-0.09
LUMO -d_{zx}	-0.17	-0.15	-0.13	-0.10
LUMO -$d_{x^2-y^2}$	0.09	0.13	0.08	0.08
LUMO -$d_{3z^2-r^2}$	0.15	0.16	0.12	0.10
d_{xy}-d_{xy} ($\parallel c$ axis)	0.05	0.02	0.03	0.03
$d_{yz(zx)}$-$d_{yz(zx)}$ ($\parallel c$ axis)	-0.06	-0.03	-0.03	-0.02
d_{xy}-d_{xy} ($\perp c$ axis)	0.01	0.01	0.01	0.01
Energy levels				
LUMO	0	0	0	0
d_{xy}	-0.98	-0.44	-0.44	-0.48
$d_{yz,zx}$	-1.56	-0.85	-0.81	-0.76

B. (DMe-DCNQI)$_2$Cu

Figure 7 shows the band structure near the Fermi level for (DMe-DCNQI)$_2$Cu. The lattice parameters and atomic positions are taken from Ref. 4 which are obtained at 20 K. Comparing the present GGA result with the previous result shown in Fig. 2(a) of Ref. 14, we can hardly see the difference between them. (DMe-DCNQI)$_2$Cu belongs to group I and it remains metallic down to 0.5 K. The shape of the four LUMO bands is very different from those of (DMe-DCNQI)$_2M$ with M=Ag or Li. Some of the four LUMO bands have significant dispersion even along the direction perpendicular to the c axis, suggesting that the hybridization between the LUMO and Cu d states is important and that the electronic structure has some 3D characters. The existence of the hybridization can be seen also in the dispersion of the d_{xy} bands, which are located about 0.2 eV below the bottom of the LUMO bands. Other d bands of Cu are located in between the d_{xy} bands and the HOMO bands of DCNQI molecules. All d bands are located between the LUMO and HOMO bands in this system. This aspect was demonstrated more clearly in our previous paper[14] by comparing the band structures between (DMe-DCNQI)$_2$Cu and the artificial system without Cu.

By comparing the present result with those of Li and Ag salts, the role of d orbitals can be understood more clearly. The band structure of (DMe-DCNQI)$_2$Li, which includes no d orbitals, is similar to that of a system with only DMe-DCNQI columns shown in our previous paper,[14] except the position of the Fermi level. The interaction between DMe-DCNQI columns is very small and unless there is significant hybridization between the LUMO and the orbitals of cation M, the band structure shows very strong 1D character. As Ag has much deeper d levels than Cu, the Ag salt has smaller $p\pi$-d hybridization than the Cu salt and the electronic structure of the Ag salt is essentially the same as that of the Li

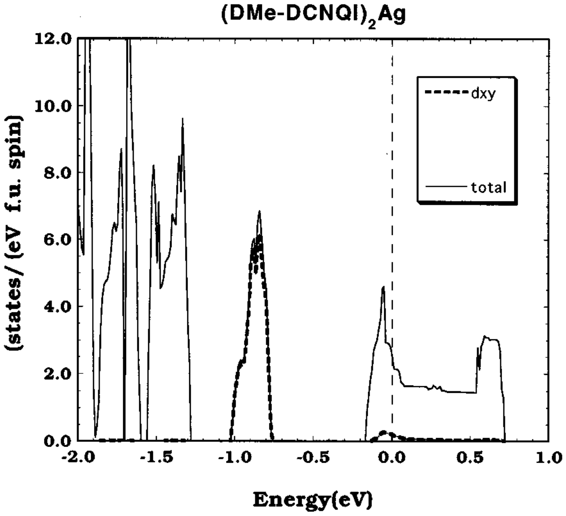

FIG. 6. Total DOS's (solid line) and projected DOS's (dashed line) onto the d_{xy} orbital of Ag for (DMe-DCNQI)$_2$Ag. The projected DOS's is obtained by the TB calculation fitted to the electronic structure of the first-principles calculation.

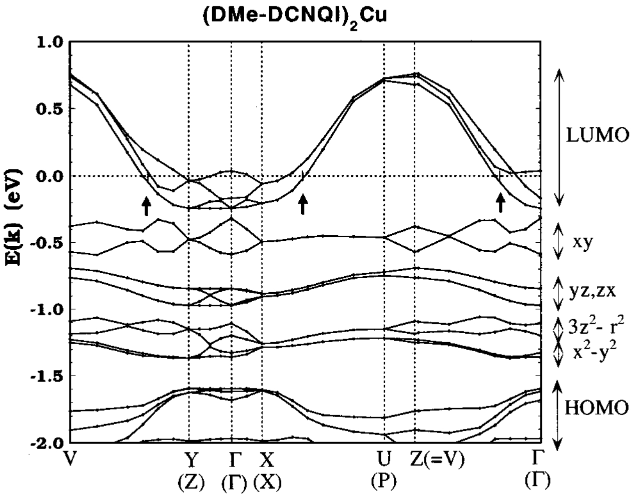

FIG. 7. Band structure of (DMe-DCNQI)$_2$Cu. The arrows along the horizontal dotted line indicate the Fermi wave vector corresponding to the CDW formation with threefold periodicity along the c axis.

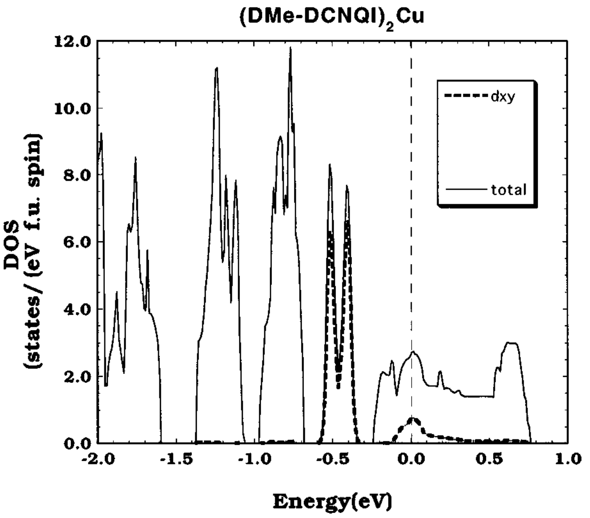

FIG. 8. Total DOS's (solid line) and projected DOS's (dashed line) onto the d_{xy} orbitals of Cu for (DMe-DCNQI)$_2$Cu. The projected DOS's is obtained by the TB calculation.

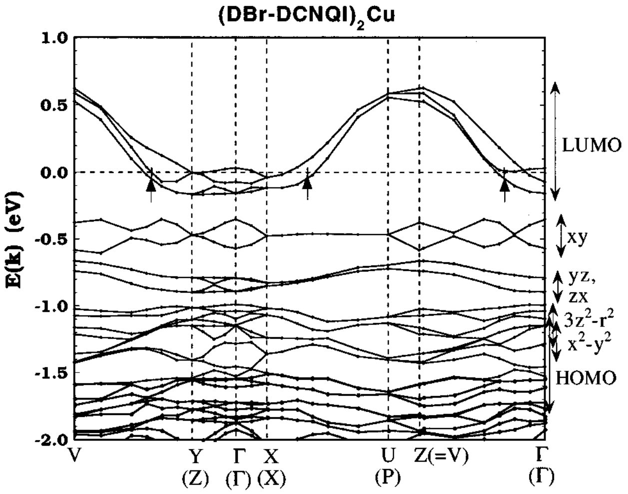

FIG. 9. Band structure of (DBr-DCNQI)$_2$Cu. The arrows along the horizontal dotted line show the Fermi wave vector corresponding to the CDW formation with threefold periodicity along the c axis.

salt.[30] This is the reason why Cu and Ag salts have such different electronic properties.

The four Fermi surfaces obtained by the TB fit are almost the same as those shown in Fig. 3 of Ref. 14. Two particularly important aspects should be noted. First, a small hole pocket around the Γ point, which is observed by the dHvA measurement, is reproduced in the present calculation. The area of the hole pocket in the $k_z=0$ plane is 35% of the first Brillouin zone in the present calculation,[31] while the observed value is 27%. Second, there exist some pieces of flat Fermi surfaces with nesting vector of approximately $\frac{1}{3}c^*$. The existence of such Fermi surfaces is consistent with the experimental fact that (DMe-DCNQI)$_2$Cu is on the verge of the instability of CDW formation with $3c$ periodicity.

The DOS's of (DMe-DCNQI)$_2$Cu and the projected DOS's onto the d levels of Cu obtained by the TB model calculation are shown in Fig. 8. The d_{xy} orbital of Cu makes an appreciable contribution to the states at the Fermi level. Again with the TB fit, the charge state of Cu is estimated to be 1.46. This value should be compared with 4/3 as the formal charge of Cu as suggested by experiments.[3,32] The DOS's value at the Fermi level, $D(E_F)$, gives the electronic specific-heat coefficient γ of 12.9 mJ/mol/K^2. The corresponding experimental value has some ambiguity, but it seems to be converging to a value[25] of about 20 mJ/mol/K^2. Similarly, the Pauli susceptibility χ estimated by the present $D(E_F)$ is 0.18×10^{-3} emu/mol and the experimental value is 0.5×10^{-3} emu/mol.[24] The calculated effective mass of the hole around the Γ point is about $2.0m_0$ with m_0 the mass of free electrons, while the experimental cyclotron mass of the dHvA oscillation is $3.5m_0$. The electron-phonon interaction and the electron-electron interaction which may be required to account for the above discrepancy by factor of 1.8–3 will be of moderate strength.

C. (DBr-DCNQI)$_2$Cu, (DI-DCNQI)$_2$Cu, and (DI-DCNQI)$_2$Li

Next we discuss the electronic structures of halogen substituted Cu and Li salts. (DBr-DCNQI)$_2$Cu belongs to the group II with the MI transition temperature $T_{\mathrm{MI}}\sim160$ K and shows physical properties typical to the Cu salt family. On the other hand, (DI-DCNQI)$_2$Cu shows very unique properties among Cu salts, as is already mentioned in Sec. II. Therefore, we will discuss in detail how and why (DI-DCNQI)$_2$Cu is unique. In the last part of this section we also present the electronic structure of the iodine substituted Li salt, (DI-DCNQI)$_2$Li and discuss how it is different from (DMe-DCNQI)$_2$Li.

The structure used in the calculation for (DBr-DCNQI)$_2$Cu is the one at room temperature and is taken from Ref. 1. Those of (DI-DCNQI)$_2$Cu and (DI-DCNQI)$_2$Li are at 9 K and 18 K, respectively.[26] The band structure of (DBr-DCNQI)$_2$Cu is shown in Fig. 9. It is qualitatively the same as that of (DMe-DCNQI)$_2$Cu: two of the four LUMO bands show 3D character and the other two show strong 1D character of cosine bands. The present band structure can be reproduced by a simple TB model with high accuracy and again we found that some pieces of Fermi surfaces are almost planar and the nesting vector associated with these Fermi surfaces corresponds to threefold CDW formation along the c axis. Note that the present calculation uses the lattice parameters and the atomic positions of the metallic phase. The strong tendency towards instability to the threefold CDW formation for the metallic phase of (DBr-DCNQI)$_2$Cu is consistent with the experimental results.

On the other hand, the band structure of (DI-DCNQI)$_2$Cu in Fig. 10 is significantly different from those of (DMe-DCNQI)$_2$Cu and (DBr-DCNQI)$_2$Cu. Figure 11 shows the DOS's of (DI-DCNQI)$_2$Cu and some of the molecular orbitals of an isolated DI-DCNQI molecule are shown in Fig. 12. We also calculated the band structure of the DI salt and that of an artificial system with only DI-DCNQI columns both by LDA. From these results, we note the following important aspects:

(1) The bandwidth of the LUMO for the DI salt is much narrower than that of DMe salt.

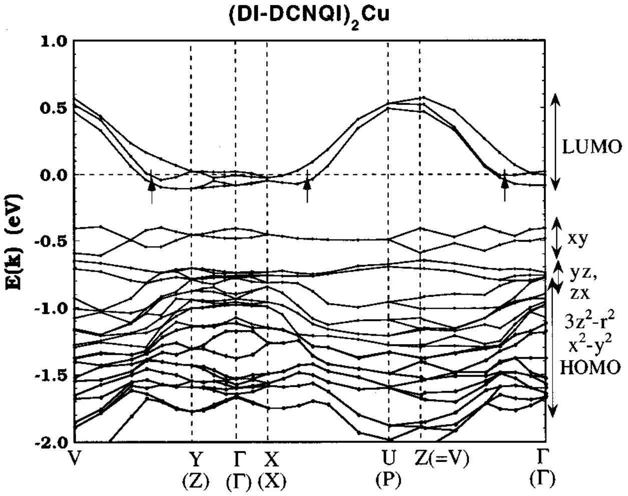

FIG. 10. Band structure of (DI-DCNQI)$_2$Cu. The arrows along the horizontal dotted line indicate the Fermi wave vector corresponding to the CDW formation with threefold periodicity along the c axis.

(2) The hybridization between the neighboring 1D LUMO bands is slightly stronger in the DI salt than in the DMe salt and all four LUMO bands show appreciable deviation from 1D cosine bands.

(3) The gap between the HOMO and LUMO bands is about 0.8 eV for the DI salt which is much reduced from 1.2 eV for the DMe salt.

(4) The $p\pi$-d hybridization in the DI salt is reduced compared with that in the DMe salt.

(5) The Fermi-surface nesting vector deviates appreciably from the commensurate one of $\frac{1}{3}c^*$ in the DI salt.

(6) The density of states at the Fermi energy of (DI-DCNQI)$_2$Cu is about twice as large as that of (DMe-DCNQI)$_2$Cu.

Aspect (1) can already be seen in the electronic structure of the system with only (DI-DCNQI) columns. The width of the LUMO band is mainly determined by the overlap between the LUMO-$p\pi$ orbitals of neighboring DCNQI molecules along the c axis. The LUMO-$p\pi$ state of the DI-DCNQI molecule has an antibonding character like that of the DMe-DCNQI molecule, as can be seen in Fig. 12(a). Therefore, the hopping integral between the neighboring LUMO-$p\pi$ orbitals will be reduced due to plus-minus cancelation in their overlap integral with the increasing of the overlap displacement (see Fig. 13) between the neighboring DCNQI molecules. In fact, the overlap displacement is the largest in the DI salt among several (DCNQI)$_2$Cu. This reduction due to plus-minus cancelation is very sensitive to the crystal structure. For example, the bandwidth of LUMO bands of (DI-DCNQI)$_2$Cu reported in our previous paper [Fig. 5(a) of Ref. 14] is smaller than the present one by 0.1 eV. This is not due to the difference between the LDA and GGA, but due to the difference in the crystal structure. In our previous paper, we used the experimental lattice parameters and atomic positions at room temperature, while those at 9 K are taken at present. The overlap of the LUMO of (DI-DCNQI)$_2$Cu estimated by the first-principles calculation with plane-wave basis sets is 53% of that of (DMe-DCNQI)$_2$Cu. This difference of the overlap integral can explain most of the difference in the LUMO bandwidth between the DI and DMe cases. On the other hand, the calculation based on the extended Hückel approximation with a localized orbital basis did not result in such a large difference: the overlap of the LUMO for the DI salt is 87% of that for the DMe salt.[33] In a subtle case where the overlap integral is determined by significant plus-minus cancelation, a very accurate treatment of the tails of molecular orbitals is required. The plane-wave basis set is more approximate than the localized orbital basis set for this purpose.

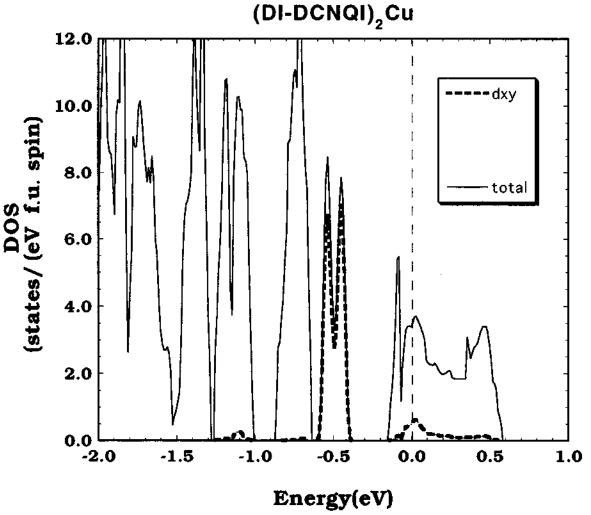

FIG. 11. Total DOS's (solid line) and projected DOS's (dashed line) onto the d_{xy} orbitals of Cu for (DI-DCNQI)$_2$Cu. The projected DOS's is obtained by the TB calculation.

Aspect (2) may correspond to the experimental observation that the anisotropy of (DI-DCNQI)$_2$Cu is small compared with those of other Cu salts. $\rho_\parallel/\rho_\perp$ in (DI-DCNQI)$_2$Cu is about 1/3, while it is about 1/10 in (DMe-DCNQI)$_2$Cu [$\rho_\parallel$ ($\rho_\perp$): the resistivity along (perpendicular to) the c axis]. Kashimura *et al.*[22] pointed out that LUMO-LUMO interchain coupling is important for this small anisotropy. We can see from Fig. 12 that the LUMO has noticeable weight on the I atom and that the weight is much larger for some occupied orbitals near the HOMO.

The hybridization between the neighboring 1D LUMO bands comes through two possible paths: one is between the I atoms and the other is the I-N$_{(2)}$ interaction (N$_{(2)}$: the N atom directly attached to the benzene ring, see Fig. 1). The intercolumn I-I and I-N$_{(2)}$ distances are only 3.63 Å and 3.49 Å, respectively. These distances are fairly short in the sense that the ionic radius of I^- is 2.16 Å. If there is a significant interaction between LUMO's of neighboring columns, the shape of the LUMO bands is not a simple cosine type [aspect (2)]. The shape of the LUMO bands is approximately reproduced by considering these intercolumn interactions. However, the detailed band structure in the $k_z=0$ plane cannot be reproduced well by the present TB model calculations. We have to consider additional interactions, for example, the effect of other orbitals which are not considered in the present simple TB model Hamiltonian. The electronic structure of (DI-DCNQI)$_2$Cu is unique also in this respect. It is suggested that the HOMO may have some significant ef-

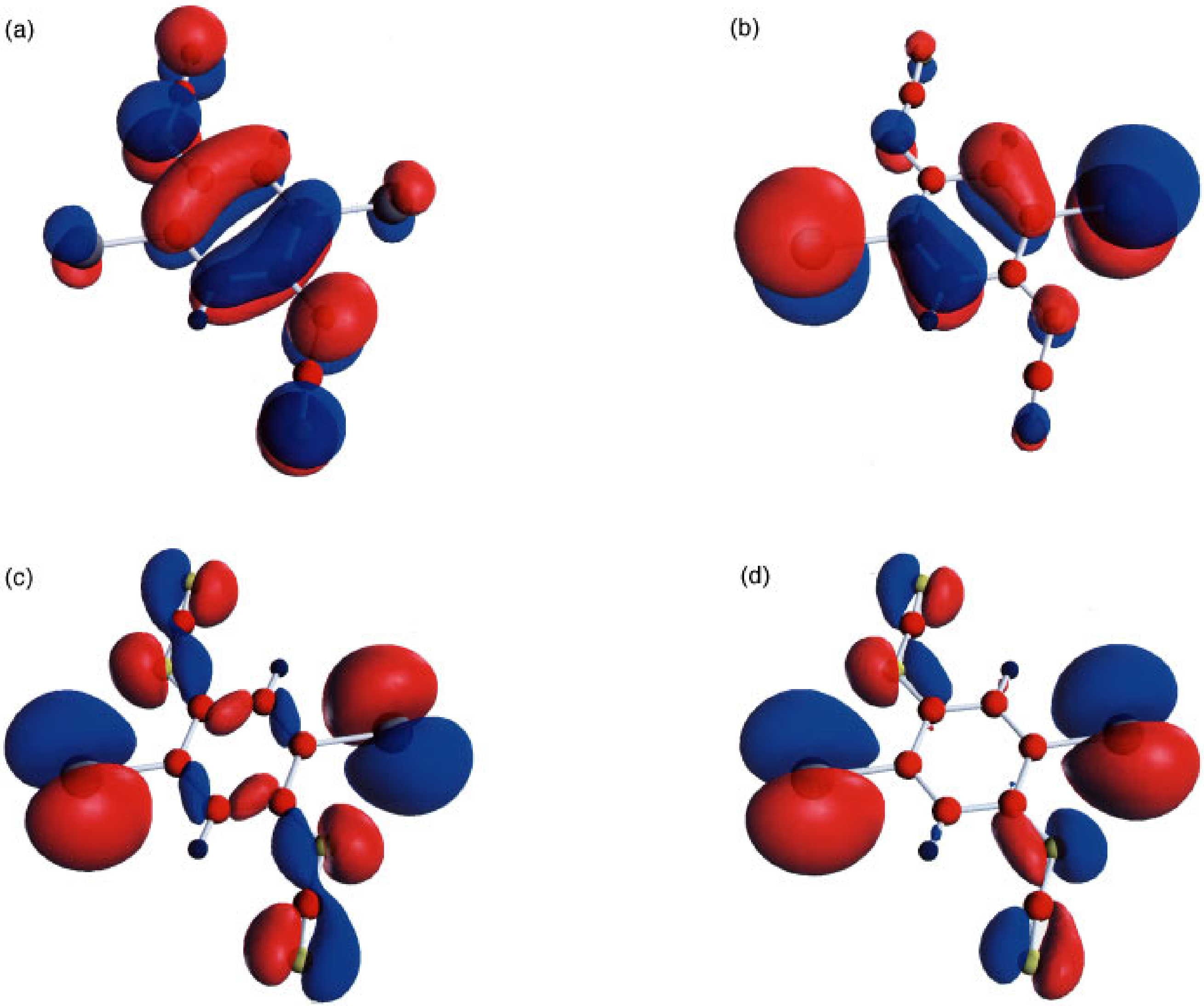

FIG. 12. Some of the molecular orbitals of DI-DCNQI. (a) 35th (LUMO), (b) 34 th (HOMO), (c) 33rd, and (d) 32nd molecular orbitals are shown. The red (blue) part indicates the region where the wave function has the positive (negative) sign.

fects because of aspect (3). Figures 14(a) and (b) compare the quality of TB fitting between DMe and DI salts.

The small HOMO-LUMO energy separation in $(\text{DI-DCNQI})_2\text{Cu}$ [aspect (3)] can be seen also in the isolated molecule, as is shown in Table III. The HOMO-LUMO energy separation in the DI-DCNQI molecule is much smaller than those of DMe-DCNQI and DBr-DCNQI molecules. From Fig. 12, the intracolumn LUMO-HOMO interaction seems to be small because of their different symmetry. However, the intercolumn LUMO-HOMO interactions may be large because the HOMO has significant weights on the I atoms and they may interact with LUMO's of neighboring columns. The effects of the HOMO are also suggested by the following analysis.

We show the electron density associated with the states whose eigenenergies are within 0.10 eV from the Fermi energy for (a) $(\text{DBr-DCNQI})_2\text{Cu}$ and (b) $(\text{DI-DCNQI})_2\text{Cu}$ in Fig. 15. By comparing these figures with that of $(\text{DMe-DCNQI})_2\text{Cu}$ (not shown here), we can see significant weights on Br and I atoms. Moreover, these weights of DI salts are appreciably larger than those of DBr salts though we cannot see such a large difference in the LUMO of isolated molecules. The interactions of I-I and I-$\text{N}_{(2)}$ between different columns seem to be important in Fig. 15(b) while the corresponding Br-Br and Br-$\text{N}_{(2)}$ interactions may not be important in Fig. 15(a). If the HOMO has some contributions to the eigenorbitals near the Fermi level, the weight on the I atom becomes larger because the HOMO has more weight on the I atom. We projected the eigenorbitals to the molecular orbitals and found that the contribution of the HOMO to the eigenorbitals near the Fermi level is much larger in $(\text{DI-DCNQI})_2\text{Cu}$ than in $(\text{DMe-DCNQI})_2\text{Cu}$ and $(\text{DBr-DCNQI})_2\text{Cu}$, although the absolute value is small: the contribution of the HOMO and its neighboring occupied orbitals to the norm of the eigenorbitals near the Fermi level is less than 1/10.

With regard to aspect (4), we first note in Table II that the $p\pi$-d_{xy} hybridization parameter $t_{p,xy}$ (LUMO-d_{xy} in Table II) in the TB fit for $(\text{DI-DCNQI})_2\text{Cu}$ is only 10% smaller than that for $(\text{DMe-DCNQI})_2\text{Cu}$. The reduction in $t_{p,xy}$ may have some origins. The N-Cu distance is about 1% larger in $(\text{DI-DCNQI})_2\text{Cu}$ than in $(\text{DMe-DCNQI})_2\text{Cu}$, leading to a

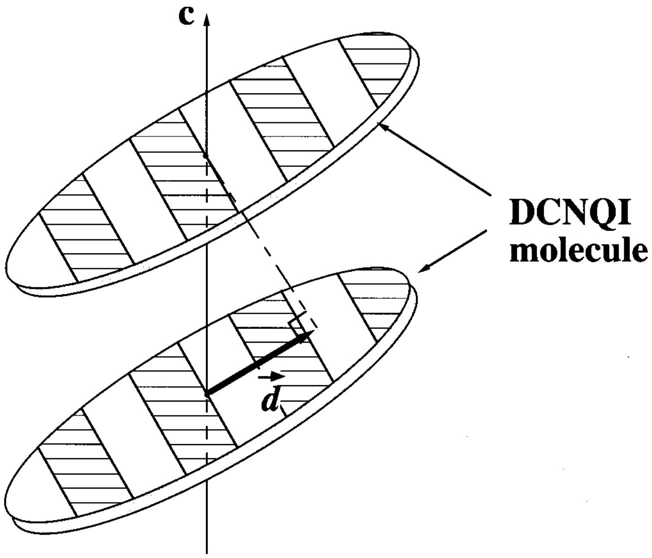

FIG. 13. A schematic diagram for the definition of the overlap displacement $\vec{d}$ between the neighboring DCNQI molecules. The blank and hatched areas denote the areas with positive and negative sign of the LUMO wave function [see Fig. 12(a)].

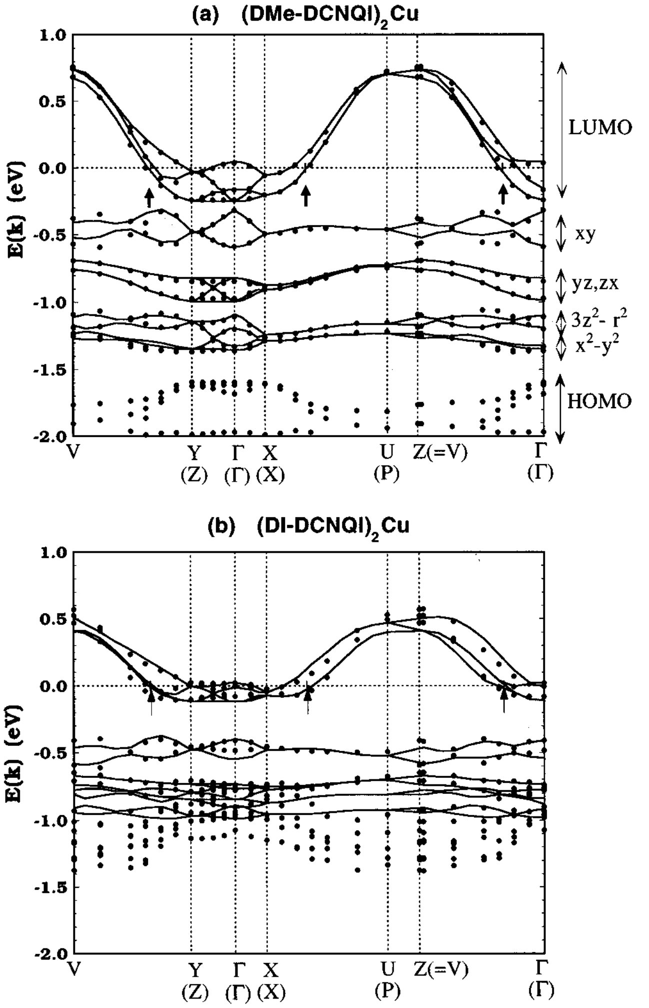

FIG. 14. Band structure of (a) (DMe-DCNQI)$_2$Cu and (b) (DI-DCNQI)$_2$Cu obtained by the TB model calculations (solid line). The dots in the figure indicate the results of the first-principles calculations.

reduction of $t_{p,xy}$ by about 4%. The mixing of the HOMO and its neighboring occupied states into the LUMO band can also contribute a few % reduction in $t_{p,xy}$, because those orbitals have a negligible weight on $N_{(1)}$. Another important reason of the reduced $p\pi$-d_{xy} hybridization is the large energy separation between the bottom of the LUMO band and the top of the d_{xy} bands for (DI-DCNQI)$_2$Cu. This energy separation is larger for (DI-DCNQI)$_2$Cu than for (DMe-DCNQI)$_2$Cu by factor 2.5, as we can see from Fig. 7 and Fig. 10. One of the reasons for this is the narrow bandwidth of LUMO [aspect(1)]. Another is the fact that the d_{xy} level is located at a lower energy because of the smaller value of α (closer to T_d symmetry, see Table I). The HOMO and its neighboring occupied states may play substantial roles in the states near the bottom of the LUMO bands for (DI-DCNQI)$_2$Cu.

As for aspect (5), the appreciable deviation of the nesting Fermi-surface vector from the commensurate one of $\frac{1}{3}c^*$ is consistent with the experimental fact that the metallic state of (DI-DCNQI)$_2$Cu is much more stable against the insulating state compared with the situation in (DMe-DCNQI)$_2$Cu.[22] Aspect (6) is a result of aspect (1). The calculated values of γ and χ are 21.9 mJ/mol/K^2 and 0.30×10^{-3} emu/mol, respectively. The corresponding experimental values[25] are 75 mJ/mol/K^2 and 0.9×10^{-3} emu/mol,[24] respectively. Again, the present calculations underestimate γ and χ to the extent similar to the case in the DMe salt.

The uniqueness of the DI case among DCNQI-Cu systems can be seen also in the Li salt. The band structure of (DI-DCNQI)$_2$Li is shown in Fig. 16. This band structure is completely different from that of (DMe-DCNQI)$_2$Li shown in Fig. 5. The four LUMO bands show a clear deviation from a

TABLE III. Energy levels (in eV) of molecular orbitals for DMe-DCNQI, DBr-DCNQI, and DI-DCNQI. The origin of energies is taken at the energy level of LUMO.

Orbital number	DMe-DCNQI	DBr-DCNQI	DI-DCNQI
30	-3.12	-2.21	-2.01
31	-2.32	-1.80	-1.53
32	-2.04	-1.63	-1.47
33	-1.96	-1.59	-1.37
34 (HOMO)	-1.79	-1.55	-1.27
35 (LUMO)	0.0	0.0	0.0
36	2.87	2.75	2.64

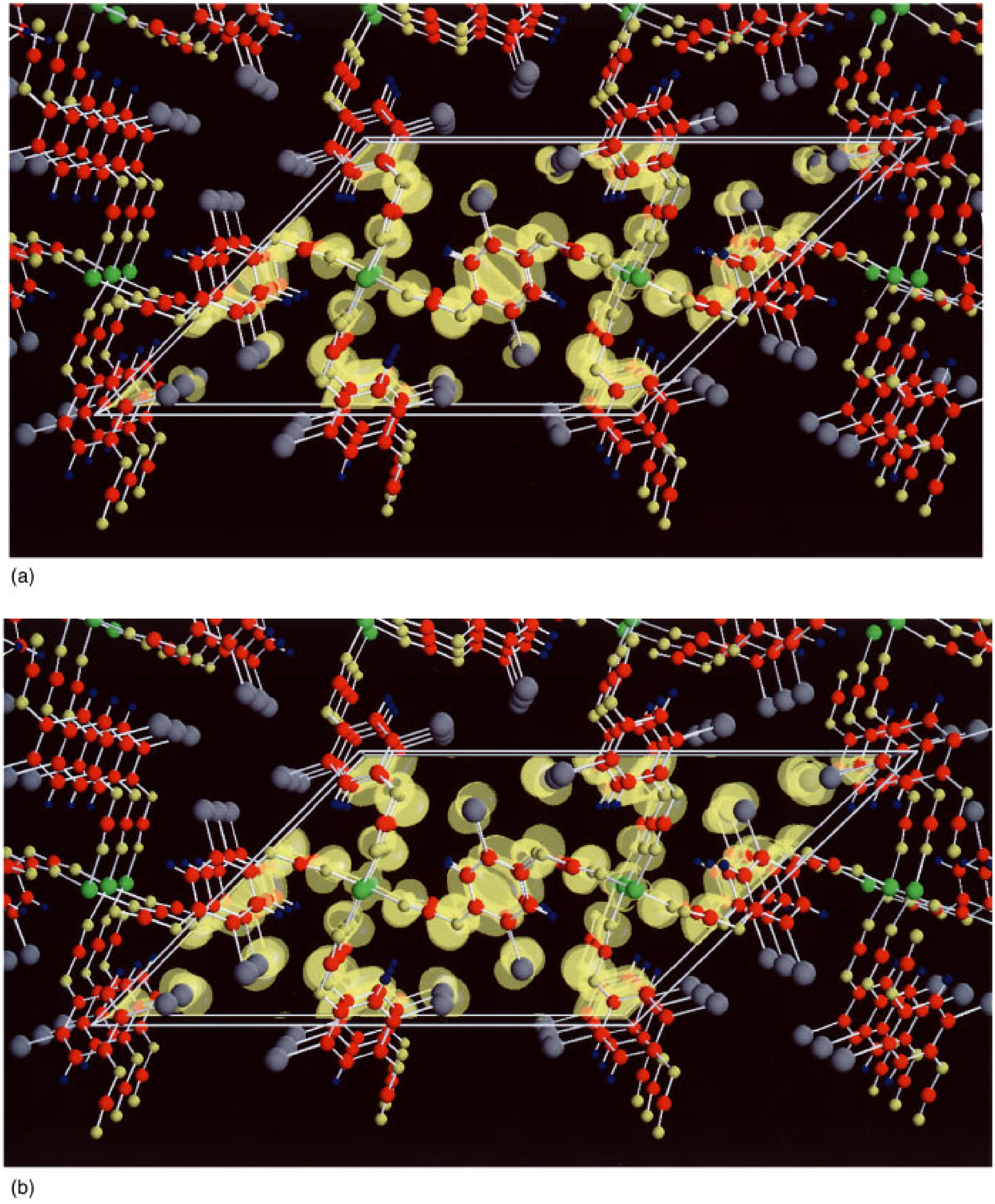

FIG. 15. Isovalue surface for the electron density associated with the states whose eigenenergies are within 0.10 eV from the Fermi energy for (a) $(\text{DBr-DCNQI})_2\text{Cu}$ and (b) $(\text{DI-DCNQI})_2\text{Cu}$.

1D cosine band though Li has no orbitals which have significant contributions to the eigenstates near the Fermi level. They show some 3D characters; the lack in degeneracy of the four LUMO bands suggests that the interaction between different columns of DCNQI molecules is significant. The arrows in Fig. 16 indicate the Fermi wave vector corresponding to the nesting vector for the fourfold periodicity. The band structure of $(\text{DI-DCNQI})_2\text{Li}$ does not show a feature of the formation of the CDW with fourfold periodicity in the present calculation. Moreover, it has a very large density of

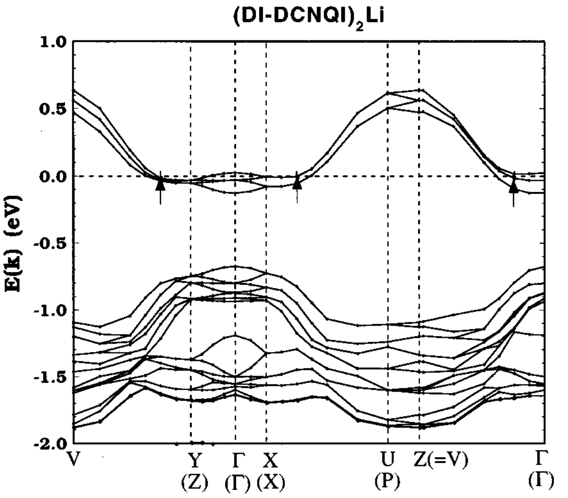

FIG. 16. Band structure of (DI-DCNQI)$_2$Li. The arrows in the figure show the Fermi wave vector corresponding to the CDW formation with fourfold periodicity along the c axis.

states at the Fermi energy, which is about 2.5 times larger than that of (DMe-DCNQI)$_2$Cu. As was mentioned in Sec. II, (DI-DCNQI)$_2$Li shows the semiconducting behavior even at room temperature, and no superstructures have been reported[26] so far. It has been recently reported that (DI-DCNQI)$_2$Ag, which shows physical properties similar to (DI-DCNQI)$_2$Li, and shows antiferromagnetic order, while other Ag or Li salts show spin Peierls transition at low temperatures, implying that DI salts have much reduced 1D characters compared with other salts.[27] At the present stage we do not have much experimental information about the physical properties of (DI-DCNQI)$_2$Li. However, it is obvious from the present calculation that (DI-DCNQI)$_2$Li has some unique features among the Li salts.

D. Supplementary discussion

There remain several works to be done. Among them we point out three important problems. First, the most interesting and important aspect to be elucidated is the nature of the insulating state of Cu salts. The first-principles calculation for the insulating phase is a very challenging task, but is too difficult to perform at the present stage. It is not only due to a large system size caused by the threefold modulation, but also due to the fundamental problem of the local spin density approximation (LSDA) and even the GGA. This is a problem similar to that for the parents compounds of high-T_C cuprates whose antiferromagnetic insulating phase has not been properly described by the LSDA band calculations. Fukuyama argued that the insulating state is realized by the Mott transition in the LUMO bands which hybridize with Cu d states, because these bands become essentially half filled when the Peierls gap opens in the other LUMO bands which have a strong tendency of CDW formation with threefold periodicity.[34] Ogawa and Suzumura analyzed the phase diagram of DCNQI-Cu systems by using the periodic Anderson model including the electron-phonon coupling.[35] In both arguments, the electron-electron interaction is considered only for the Cu d states. However, as was mentioned in Sec. II, the LUMO of a DCNQI molecule has a strong electron-electron interaction. This was more directly confirmed by a recent experiment.[36] As the states near the Fermi level are dominated by the LUMO of DCNQI molecules, the electron-electron interaction in the LUMO has to be included in model calculations.

Second, we would like to compare our results with the recent photoemission (PE) measurement by Sekiyama *et al.* for the metallic state of deuterated (DMe-DCNQI)$_2$Cu.[37] Their PE spectrum has a vanishingly small intensity near the Fermi level and they attributed this feature to the characteristics of the Tomonaga-Luttinger (TL) liquid.[38,39] However, the present calculation suggests that the effective intercolumn interaction is an order of 0.1 eV which may be large enough to destroy the characteristic behavior of the TL liquid near the Fermi level. In order to solve the discrepancy between the present calculation and the PE measurements, a study on the electronic structures near the surface may be required.

Third, the present calculations have confirmed the uniqueness of I as substituents. Experimentally, the second metallic phase appears under pressure beyond 20 GPa for (DI-DCNQI)$_2$Cu and this metallic phase seems to have a different character from the one in the normal pressure.[22] The elucidation of the basic nature of the second metallic phase is an interesting subject of theoretical study. However, the detailed crystal structure under pressure is not easy to determine experimentally for organic solids with many atoms per unit cell. Therefore, the crystal structure has also to be determined theoretically. This is now a feasible task and will be discussed in a forthcoming paper.

V. CONCLUDING REMARKS

We have performed the electronic structure calculations based on a GGA for the metallic states of the organic solids (2,5-R_1,R_2-DCNQI)$_2M$ with the following combination of R_1,R_2 and M: for M=Cu, R_1=R_2=CH$_3$, Br, I; for M=Li, R_1=R_2=CH$_3$, I; for M=Ag, R_1=R_2=CH$_3$. The main results are as follows:

(1) For M=Li and Ag and R_1=R_2=CH$_3$, the LUMO bands are essentially 1D like and the Fermi surfaces show a strong tendency of formation of a CDW with fourfold periodicity along the c axis.

(2) For M=Cu and R_1=R_2=CH$_3$ and Br, the $p\pi$-d hybridization is strong enough to produce a small 3D Fermi surface. The calculated size of the Fermi surface for R_1=R_2=CH$_3$ agrees well with the experimental result.

(3) For M=Cu and R_1=R_2=CH$_3$ and Br, the Fermi surfaces produced by two (among four) LUMO bands show a strong tendency of formation of a CDW with a threefold periodicity along the c axis.

(4) The qualitative difference between the Ag and Cu salts comes from the difference in the energy level of d states: Ag has a deeper d level so that the $p\pi$-d hybridization is weak.

(5) The systems with R_1=R_2=I are rather unique among several DCNQI systems. The unique features are caused by three reasons. First, the large ionic size of I$^-$ produces an appreciable interaction between neighboring DCNQI columns. Second, the LUMO bandwidth is much narrower compared with those for other substituents. Third, the Fermi

wave vectors deviate appreciably from the commensurate nesting wave vectors, $c^*/3$ for (DI-DCNQI)$_2$Cu and $c^*/4$ for (DI-DCNQI)$_2$Li.

In this paper, we discussed the variety in the electronic structure of $(R_1,R_2\text{-DCNQI})_2M$ for different choices of substituents R_1, R_2 and metallic elements M. Another interesting aspect in the electronic structure of the DCNQI-Cu systems is that it is very sensitive to the crystal structure. We will discuss this point in the next paper together with the subject about the accuracy of theoretical determination of the crystal structure.

ACKNOWLEDGMENTS

We thank Professor R. Kato, Dr. H. Sawa, Professor H. Kobayashi, and Professor A. Kobayashi for providing us with experimental information. We thank also Professor K. Kanoda for the experimental information about (DI-DCNQI)$_2$(Li,Ag) and Professor H. Fukuyama for valuable comments on the insulating phase of the Cu salts. Thanks are also given to Dr. N. Hamada, Dr. Y. Morikawa, and Dr. T. Yamasaki for their useful advice and help in many aspects of performing the calculations and analyses. This work was partially supported by the Grant-in-Aid for Scientific Research on the priority area, Novel Electronic States in Molecular Conductors, from the Ministry of Education, Science and Culture. The calculations were performed by the JRCAT Supercomputer System. The financial support from the New Energy and Industrial Technology Development Organization (NEDO) is gratefully acknowledged.

---

*Present Address, National Research Institute for Metals, 1-2-1 Sengen, Tsukuba, Ibaraki 305, Japan

[1] R. Kato, H. Kobayashi, and A. Kobayashi, J. Am. Chem. Soc. **111**, 5224 (1989).

[2] S. Hünig and P. Erk, Adv. Mater. **3**, 225 (1991).

[3] H. Kobayashi *et al.*, Phys. Rev. B **47**, 3500 (1993).

[4] K. Sinzger *et al.*, J. Am. Chem. Soc. **115**, 7696 (1993).

[5] T. Mori *et al.*, Chem. Lett. **1984**, 957 (1984).

[6] S. Uji *et al.*, Phys. Rev. B **50**, 15 597 (1994).

[7] R. O. Jones and O. Gunnarsson, Rev. Mod. Phys. **61**, 689 (1989).

[8] J. P. Perdew, in *Electronic Structure of Solids '91*, edited by P. Ziesche and H. Eschrig (Akademie-Verlag, Berlin, 1991).

[9] O. K. Andersen, Phys. Rev. B **12**, 3060 (1975).

[10] A. R. Williams, J. Kübler, and J. C. D. Gelatt, Phys. Rev. B **19**, 6094 (1979).

[11] J. Kübler, M. Weger, and C. B. Sommers, Solid State Commun. **62**, 801 (1987).

[12] R. Car and M. Parrinello, Phys. Rev. Lett. **55**, 2471 (1985).

[13] D. Vanderbilt, Phys. Rev. B **41**, 7892 (1990).

[14] T. Miyazaki, K. Terakura, Y. Morikawa, and T. Yamasaki, Phys. Rev. Lett. **74**, 5104 (1995).

[15] Y.-N. Xu, W. Y. Ching, Y. C. Jean, and Y. Lou, Phys. Rev. B **52**, 12 946 (1995).

[16] R. Moret, Synth. Met. **27**, B301 (1988).

[17] S. Hünig *et al.*, Angew. Chem. Int. Ed. Engl. **31**, 859 (1992).

[18] S. Aonuma, H. Sawa, R. Kato, and H. Kobayashi, Chem. Lett. **1993**, 513 (1993).

[19] S. Tomiĉ, D. Jèrome, A. Aumüller, and J. U. Schütz, J. Phys. C **21**, L203 (1988).

[20] T. Mori *et al.*, J. Phys. Soc. Jpn. **56**, 3429 (1987).

[21] K. Yakushi *et al.*, Mol. Cryst. Liq. Cryst. **181**, 217 (1990).

[22] Y. Kashimura *et al.*, Solid State Commun. **93**, 675 (1995).

[23] Y. Kashimura *et al.* (unpublished).

[24] M. Tamura *et al.*, Solid State Commun. **93**, 585 (1995).

[25] Y. Nishio (unpublished).

[26] H. Sawa (private communications).

[27] K. Hiraki and K. Kanoda (unpublished).

[28] N. Troullier and J. L. Martins, Phys. Rev. B **43**, 1993 (1991).

[29] R. Kato, H. Kobayashi, and A. Kobayashi (private communications).

[30] Although the main source of the difference of the electronic structures between Ag and Cu salts comes from the positions of their d levels, it cannot be determined by their atomic levels. Atomic d levels of Ag are deeper than those of Cu by 2.3 eV in LDA. This value is larger compared with that in solids: the difference of d_{xy} levels between Ag and Cu salts is about 0.5 eV. The d levels of Ag or Cu strongly depend on both the crystal field and the charge state, which must be obtained by the self-consistent calculations for solids.

[31] In our previous paper (Ref. 14) we used the LDA instead of the GGA and the calculated area was 29%.

[32] I. H. Inoue *et al.*, Phys. Rev. B **45**, 5828 (1992).

[33] The calculation of the overlap was done for the structure at room temperature (Ref. 22).

[34] H. Fukuyama, J. Phys. Soc. Jpn. **61**, 3452 (1992).

[35] T. Ogawa and Y. Suzumura, Phys. Rev. B **51**, 10 293 (1995).

[36] A. Tanaka *et al.*, Phys. Rev. B **52**, 7951 (1995).

[37] A. Sekiyama *et al.*, Phys. Rev. B **51**, 13 899 (1995).

[38] S. Tomonaga, Prog. Theor. Phys. **5**, 544 (1950).

[39] J. M. Luttinger, J. Math. Phys. **4**, 1154 (1963).

[40] C. J. Bradley and A. P. Cracknell, *The Mathematical Theory of Symmetry in Solids* (Clarendon Press, Oxford, 1972).